

Article

Characterizing Temporal Dynamics of Urban Heat Island in a Rapidly Expanding City: A 39 Years Study in Zhengzhou, China

Huawei Li ¹, Sandor Jombach ², Guohang Tian ¹, Yuanzheng Li ³ and Handong Meng ^{4,5,*}¹ College of Landscape Architecture and Art, Henan Agricultural University, Zhengzhou 450002, China² Department of Landscape Planning and Regional Development, Institute of Landscape Architecture, Urban Planning and Garden Art, Hungarian University of Agriculture and Life Sciences, 1118 Budapest, Hungary³ School of Resources and Environment, Henan University of Economics and Law, Zhengzhou 450046, China⁴ Henan Provincial Climate Centre, Zhengzhou 450003, China⁵ CMA•Henan Key Laboratory of Agrometeorological Support and Applied Technique, Zhengzhou 450003, China

* Correspondence: menghd752@126.com

Abstract: Extreme heat wave weather phenomena have erupted worldwide in recent years. The urban heat island (UHI) effect has exacerbated urban heat waves with serious consequences for urban energy and residents' health. Therefore, a better understanding of the dynamics of the UHI effect and the influencing factors is needed in the context of carbon neutrality and global warming. This study used long-term observation and statistical data to investigate the urban heat island intensity (UHII) over the past 39 years (1981–2019) and to analyze the temporal changes of the UHI effect and the relationship between the UHI effect and indicators of rapid urbanization in Zhengzhou, China. The results showed that Zhengzhou is warming 2.2-times faster than the global land warming trend of about +0.9 °C from 1981 to 2019. There is a clear phase characteristic of the heat island effect in Zhengzhou, and it offers a rapid upward trend after 2000 and a positive correlation with the urbanization process; it was found that the social and economic conditions of urban expansion in Zhengzhou have a significant relationship with UHII. We also found that the denser the urban built-up area, the more obvious the heat island effect. Compared with other countries, the influence of national policies on urban development is an indirect factor influencing the change of UHI specifically for Chinese cities. This research could provide a reference for understanding the temporal dynamics of UHI in an expanding large city for sustainable urban planning and mitigating urban warming and environmental problems.



Citation: Li, H.; Jombach, S.; Tian, G.; Li, Y.; Meng, H. Characterizing Temporal Dynamics of Urban Heat Island in a Rapidly Expanding City: A 39 Years Study in Zhengzhou, China. *Land* **2022**, *11*, 1838. <https://doi.org/10.3390/land11101838>

Academic Editor: Nir Krakauer

Received: 21 September 2022

Accepted: 17 October 2022

Published: 19 October 2022

Publisher's Note: MDPI stays neutral with regard to jurisdictional claims in published maps and institutional affiliations.



Copyright: © 2022 by the authors. Licensee MDPI, Basel, Switzerland. This article is an open access article distributed under the terms and conditions of the Creative Commons Attribution (CC BY) license (<https://creativecommons.org/licenses/by/4.0/>).

Keywords: urban heat island; air temperature; urbanization; socioeconomic indicators; local climate change; China

1. Introduction

In the current summer of 2022, extreme weather phenomena have occurred frequently around the world, with many cities in China experiencing urban heat waves (HW) and record high temperatures, and the European region experiencing the most severe drought weather in 500 years [1]. Climate change is seriously affecting world food security and human health. The frequency of extreme weather can be attributed to global warming caused by climate change and human activities.

Human activities induced by urbanization are an important factor affecting climate change. It is predicted that, by 2050, the proportion of the world's urban population will exceed 66% [2]. Rapid urbanization has resulted in expanding impervious urban areas and replacing the original natural vegetation. In contrast, human and production activities have altered the material and energy balance near the urban surface, and many environmental problems have arisen in cities [3]. According to studies [4–6], the urban heat

island effect exists in most cities worldwide, regardless of their latitude, size, topography, or climatic zone. European studies showed that heat waves and heat islands are related to geographic location, with cities at higher latitudes more susceptible to heat waves [7]. Phoenix experienced a 0.47 °C per decade minimum temperature rise from 1960 to 2000. In New York, the Central Park atmospheric UHI strength increased from 2.0 °C in 1900 to 2.5 °C by 2000 [8]. In Asia, a study of large cities based on surface temperatures showed a trend toward urban warming [9]. The average heat island intensity in Seoul, South Korea, increased by 1.3 °C from 1962 to 2017 [10]. In North China, due to urbanization, the surface temperature of large cities increased by an average of 0.16 °C per decade [11]. Nevertheless, studies also found that urban heat islands are related to demographic and climatic factors [12].

Luke Howard discovered urban heat island (UHI) in 1818, which refers to the phenomenon in which cities are warmer than rural areas [13]. Studies are usually divided into surface UHI (SUHI) and atmospheric UHI, both of which can be used to measure and define the intensity of the UHI [14]. The conventional method is based on the temperature readings of urban and rural fixed weather stations, and the calculation is based on air temperature [15]. The urban canopy layer (UCL) is the portion of the near-surface layer where urban residents live, extending from the ground to treetops and roofs [15–17]. The UCL thermal environment is highly heterogeneous and heavily influenced by human activities. Although the surface temperature is widely used to study urban heat island research, because there are many high-rise buildings in the city, the temperature reflected by remote sensing images in the building area is often the temperature on the roof of the building, and the temperature near the surface is not available. Therefore, this paper selected weather station data, and the temperature sensor was generally about 1.5 m away from the ground surface, which represents the temperature of the urban canopy layer.

Although the era of global warming has increased temperatures in both urban and rural areas [17], urbanization has contributed more to the rise in urban temperatures [18–20]. China has a rapid urbanization growth [21,22] that is even denser than other western nations (US and EU). In light of this, we examined the dynamic changes in urban and rural temperatures in Zhengzhou over the past 39 years (1981–2019). Previous papers on Zhengzhou studies on heat islands were generally based on surface temperature data from remote sensing images, which do not reflect temperature trends over time [23–28]. More importantly, the variation of nighttime temperatures in urban and rural areas is unavailable through conventional remote sensing methods. This article examined two main sections: (a) utilizing long-term observation data to analyze and characterize the temporal characteristics of UHIs; (b) using statistical socio-economic development indicators to assist the investigation and interpret UHI features. We intended to answer the following research questions:

- (1) What kind of changes in urban local climate change and UHI are observed with rapid urbanization in Zhengzhou city?
- (2) What are the differences between daytime UHI and nighttime UHI?
- (3) What are the most important urban development indicators (GDP, population density, and urbanization rate) associated with the urban heat island in Zhengzhou?

2. Study Area

Zhengzhou (34°16′–34°58′ N, 112°42′–114°14′ E) is the provincial capital of central China's Henan Province. It is situated south of the Yellow River and in the North China Plain (Figure 1). It is among China's largest transportation hubs. According to the 2021 census (<http://tj.zhengzhou.gov.cn/>, accessed on 6 June 2022), the city's total area is 7446.2 km², and its population is approximately 12,742,000. Zhengzhou's central city has the second highest population density among Chinese cities. Zhengzhou is located in the northern warm temperate zone and has a warm climate; it has four distinct seasons: a dry spring (March–May) and a hot and rainy summer (June–September). The GDP in 2021 was USD 0.18 trillion.

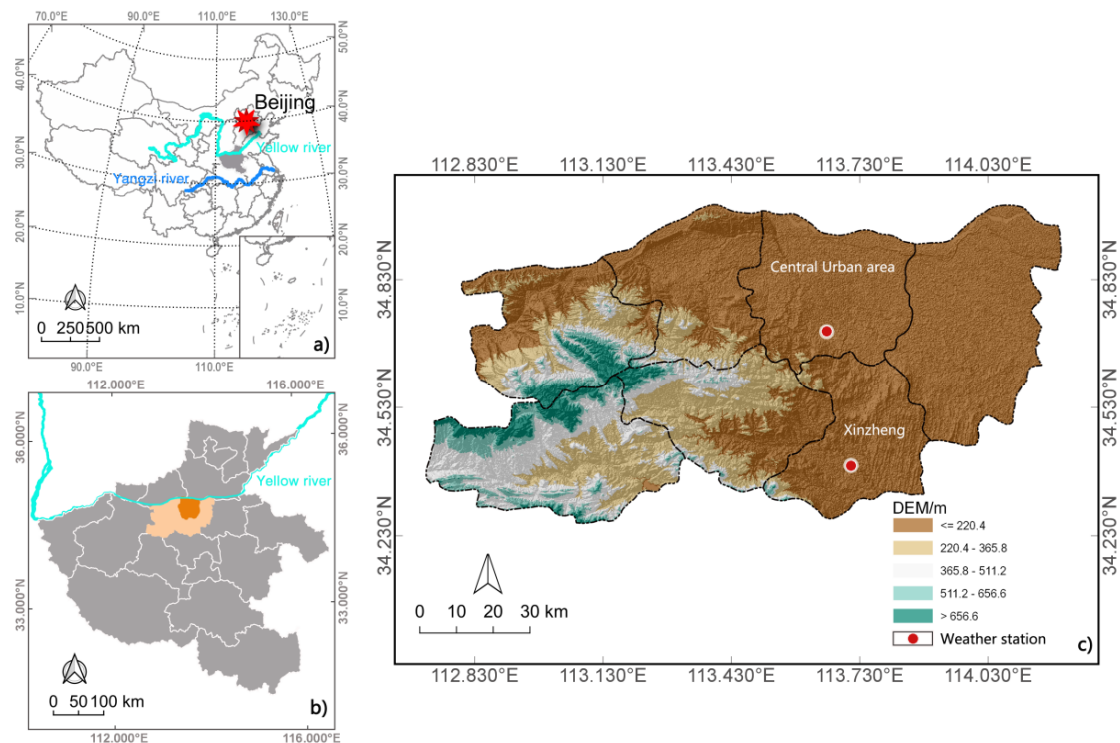


Figure 1. Location of the study area: (a) Henan province in China, (b) Zhengzhou in Henan province, and (c) Zhengzhou DEM map and weather stations.

As one of the 13 emerging megacities in China in the July 2012 Economist Intelligence Unit report, Zhengzhou has seen rapid urbanization over the past few decades. The population of Zhengzhou increased from 4.2 million in 1978 to 12.742 million in 2021. With six districts, five county-level cities, and one county within the administrative division of Zhengzhou, it is estimated that the population of Zhengzhou's central city is 1.5-times larger than the combined population of the six surrounding cities and counties. In recent years, it has been influenced by policies. For example, the Zhengzhou metropolitan area is the core area of the Central Plains Economic Zone. In addition, the national central government officially named it the eighth national central city in 2017. This national-level policy provides a wealth of opportunities for the development of Zhengzhou. The central city is developing rapidly, but the surrounding countryside lags and is dominated by agriculture. The urban-rural dual structure is extremely unbalanced, and the central city shows a high degree of agglomeration.

3. Data Sets and Method

3.1. Air Temperature Data

To examine the long-term urban heat island (UHI) and urban local climate change, this study analyzed the temporal trends of the air temperature-based UHI using observations from fixed meteorological stations at the Henan Provincial Climate Center and Zhengzhou Meteorological Bureau. In the region of Zhengzhou, two stations (with an elevation difference of around 6.2 m) have maintained meteorological data records for almost 40 years. The urban station is located in the southern portion of the core region of Zhengzhou (34.72 N, 113.65 E; 110.4 m above sea level) and can represent the urban temperature. The other station is situated in a rural location and measures temperatures in rural areas. Approximately 35 km separates the urban station from the Xinzheng station (34.38 N, 113.72 E; 116.6 m height). Rapid urbanization has resulted in environmental changes surrounding the urban weather station. According to the classification of local climate zones (LCZs) [29–31], the urban station changed from LCZ D (low plants, prior to 2000) to LCZ 6 (open low-rise), LCZ 4 (open high-rise), and LCZ 1 (compact high-rise, Table A1).

Xinzheng station's LCZ classification changed from LCZ D (before 2009) to LCZ 6 and LCZ 4 (Table A2). These two stations are national meteorological stations (Figure 1), and the meteorological data are standardized for correction and processing. The statistics on temperatures range from 1981 to 2019.

3.2. Additional Data

This study gathered official secondary data, such as urbanization index: urban population, urbanization rate, etc., from the Urban Statistics Bureau (Zhengzhou Bureau of Statistics <http://tjj.zhengzhou.gov.cn/>, accessed on 6 June 2022) and applied these socioeconomic data to assess the correlation with UHI. The data range from 1981 to 2019 and consist of socioeconomic census statistics for each year in the research area, including urbanization rate, urban population, population density, GDP, and built-up area (Table A3).

3.3. Method

3.3.1. Urban Heat Island Intensity

The formula for calculating UHI intensity (*UHII*) is as follows [32]:

$$UHII = T_u - T_r \quad (1)$$

where (a) T_u is the air temperature at the city station, and (b) T_r is the air temperature at the Xinzheng station (b). When $UHII > 0$, it means that the temperature of the urban area is higher than that of the rural area, and the heat island phenomenon occurs in this area. When $UHII \leq 0$, the region has no urban heat island phenomenon.

The annual and seasonal variations in UHI intensity were assessed using the yearly average temperature and seasonal average temperature. The four seasons were divided into spring (March to May), summer (June to August), autumn (October to November), and winter (December to February) based on the climatic zone of the study area (December to February). Additionally, the yearly average hourly temperature was used to investigate the hourly UHI intensity at various times of the day. In terms of understanding the diurnal UHI intensity and evaluating the diurnal change of *UHII* in various seasonal settings, four distinct hourly data sets (2 am, 8 am, 2 pm, and 8 pm) were selected.

3.3.2. Index of Urban Growth

The urban compactness ratio (*UCR*) is a significant metric representing urban morphology [19,33,34] and is a significant indication of the density of built-up regions, which is calculated by Equation (2):

$$UCR = 2 \frac{\sqrt{\pi A}}{P} \quad (2)$$

where A is the area of urban build-up land, and P is the perimeter of the urban boundary contour. *UCR* ranges from 0 to 1; a higher value indicates a more compacted shape, and a value closer to 1 indicates that the urban built-up land has a higher occupation and vice versa. In general, if urban land expansion changes in an infilling way, the concavity of urban edges will decrease because the urban internal gaps are gradually filled up, and, as a result, the urban form tends to be more compact.

3.4. Analysis Methods and Tools

This study was based on long-term meteorological data and urban statistics, mainly using statistical analysis software to graph and illustrate the urban temperature change, *UHII* trends, and characteristics. The main methods were correlation analysis and linear regression analysis. In this way, the interactions of the relevant factors were investigated.

4. Results

4.1. Urban Climate Change

Two weather stations' temperature data indicated that the city is warming up quickly. Figure 2 shows that, over the past 39 years, temperatures in both urban and rural areas have increased, but the increase in urban temperatures ($R^2 = 0.82$) has been more pronounced. The average urban temperature (Zhengzhou station) rose $0.67\text{ }^\circ\text{C}$ per decade from 1981 to 2019, while the average rural temperature (Xinzheng station) rose $0.43\text{ }^\circ\text{C}$ per decade. This result is consistent with a prior investigation [11]. Over forty years, the temperature raised by about $1.96\text{ }^\circ\text{C}$. In comparison to the global land warming trend of $+0.9\text{ }^\circ\text{C}$ [35], Zhengzhou has warmed up 2.2-times quicker between 1981 and 2019.



Figure 2. Mean annual temperatures were recorded at two weather stations between 1981 and 2019.

The vertical shift of the two lines in the left panel of Figure 2 shows that the temperature difference between urban and rural sites was insignificant until 2000. However, there is a noticeable increase in the upper curve after 2000, particularly after 2005, compared to the other lower curve, indicating that the temperature difference between urban and rural areas is growing and the intensity of the heat island is increasing. This is because, prior to 2000, both urban and rural stations had the same LCZ 4. Due to the rapid urbanization that occurred after 2000, the environment at urban stations changed (Tables A1 and A2), and the increase in urban temperatures was greater than that in rural areas (Figure 2). Additionally, earlier research [36] demonstrated that urbanization is one of Zhengzhou's main causes of urban warming.

4.2. Temperature-Based Temporal Dynamics of UHI Intensity

The annual mean temperatures in urban and rural areas are a direct foundation for defining Zhengzhou's atmospheric UHI. Figure 3 depicts the air temperature-based seasonal atmospheric UHI. With the highest UHI reaching $1.2\text{ }^\circ\text{C}$ (2017) and the second highest reaching $1.15\text{ }^\circ\text{C}$, it is noticeable that the urban heat island effect has significant variability, demonstrating a significant atmospheric UHI phenomenon after the turn of the century (2000). It is worth pointing out that, prior to 2000, the atmospheric UHI values were primarily negative, indicating that the annual average temperature in urban areas

was lower than in rural areas and that, consequently, the absence of heat islands during this time (1981–1999) should not have had a significant impact on local climate change.



Figure 3. Averages of the atmospheric UHI intensity (UHII) in Zhengzhou from 1981 to 2019 by year and season.

In general, the summer (mean atmospheric UHII of 0.64 °C) and spring (mean atmospheric UHII of 0.51 °C) were the strongest atmospheric UHIs of the year in Zhengzhou, with clear seasonality. Winter had the lowest UHII (mean atmospheric, at −0.11 °C). Additionally, autumn exhibited a slight heat island effect (mean atmospheric UHII of 0.1 °C). The annual average UHI mentioned earlier was consistent with the highest atmospheric UHII for the summer heat island, which was 1.7 °C (occurring in 2010 and 2011, respectively). The seasonal atmospheric UHII is now almost always above zero, even in the winter, which is significant to note. From the results, the UHI was negative in winter and autumn and positive in spring and summer, considering the effect of tree defoliation on temperature. Trees tend to cool down during the day [37,38] but keep the object warm at night due to thermal radiation. To explain this trend, further information on the change in vegetation types around urban areas is required. It can also be seen from the figure that the UHI of Zhengzhou showed a decreasing trend from 1981 to 2000, and some investigation of historical meteorological data and a comparative analysis of land cover changes are warranted in the next stage of the study.

4.3. Diurnal Variations in Atmospheric UHI Intensity across the Four Seasons

The Zhengzhou atmospheric UHIs exhibited a distinct temporal characteristic. The annual average results in Figure 4 demonstrated that the atmospheric UHII exhibits temporal variations during the day and at night. Prior to 2000, however, only the atmospheric UHI during the day was positive, while the nighttime was negative. Additionally, the atmospheric UHII during the day and night exhibited a sharp increase after 2000. The strongest atmospheric UHII in 2010 occurred at 8:00 pm.

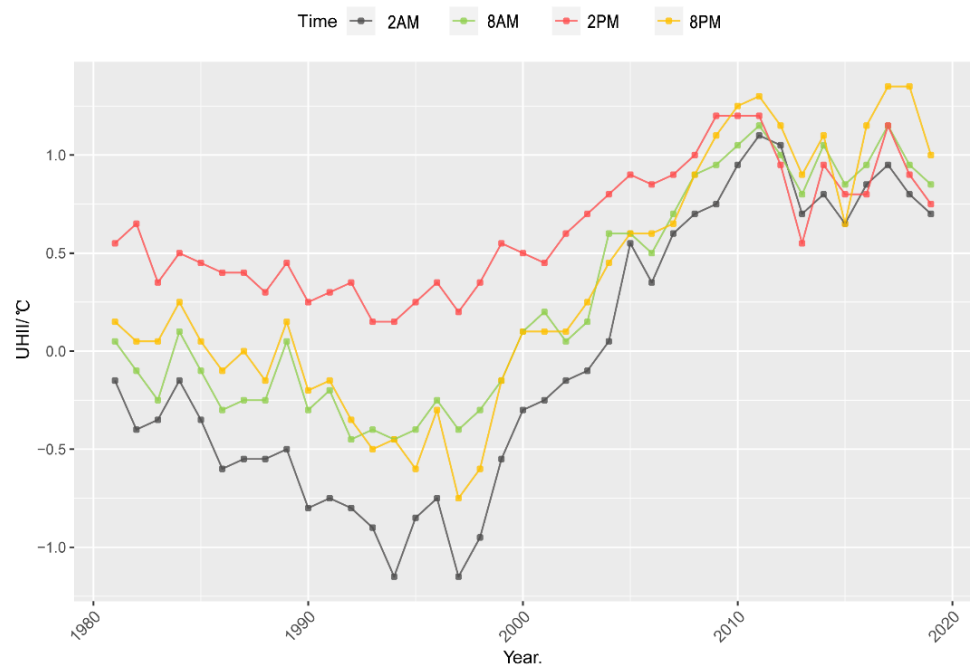


Figure 4. Mean atmospheric UHI intensity (UHII) each year at different daytime and nighttime hours in Zhengzhou over the past years (1981–2019).

In terms of the seasonal dimension (Figure 5), over the past 39 years, the heat island effect has been present both during the day and at night in all four seasons. The heat island intensity was highest during the daytime hours of 2 pm (mean 0.616 °C) and 8 pm (mean 0.318 °C) and lowest during the early hours of 2 am (mean −0.036 °C) of the four time periods chosen for this study.

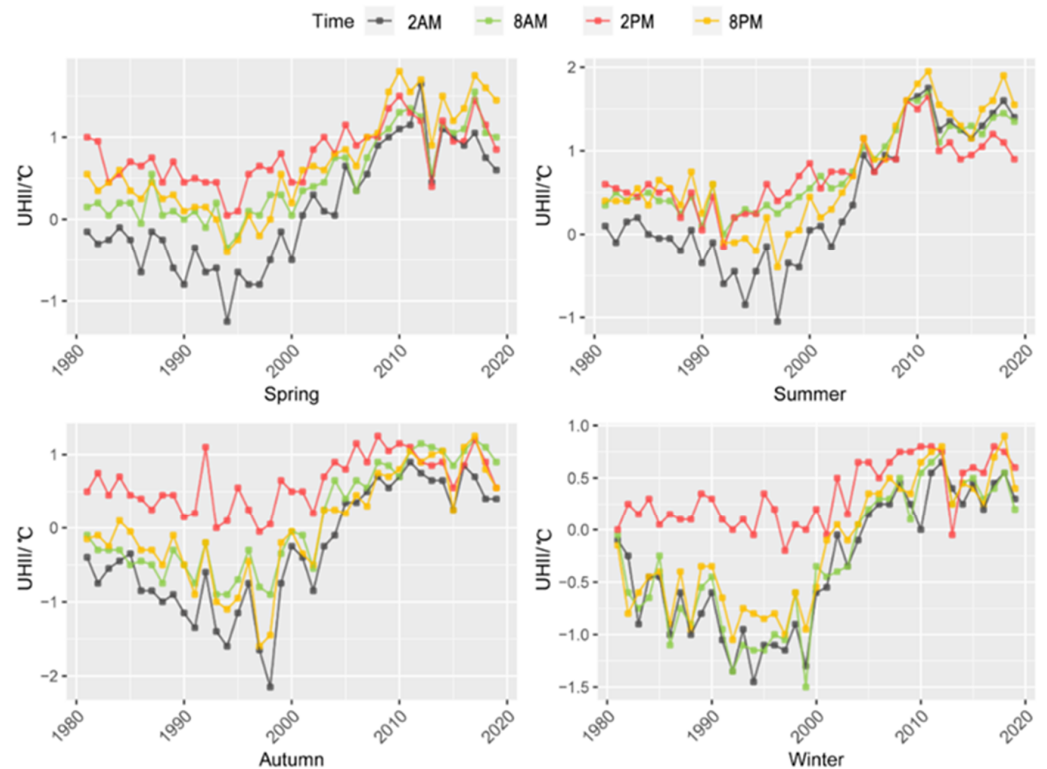


Figure 5. Characteristics of four-season hourly mean variations in atmospheric UHI intensity (1981–2019).

The diurnal heat island effect was also prominent in all seasons, and, in the summer and spring, the heat island intensity was greater, indicating a lower heat island effect during the day than at night. Autumn and winter experienced the opposite, but with a diminished heat island intensity. Summer is the season in which the heat island effect was most pronounced. Since the heat island effect was present in all three periods except for early morning (2 am), the average value of the four time periods during the summer was 0.65 °C, and the maximum atmospheric UHII was 1.95 °C (2011). The UHII at 2 pm was the most significant. In general, the diurnal heat island of the atmospheric UHII exhibited an upward trend over time, with urban temperatures consistently exceeding rural temperatures after the year 2000. Spring had the most pronounced diurnal heat island effect among the four seasons. The maximum UHII in the atmosphere during the spring season in 2010 was 1.8 °C, which is slightly lower than the summer season maximum. The average values for the four autumn and winter periods were 0.11 °C and −0.1 °C, respectively.

4.4. The Correlation between Atmospheric UHI Intensity and Urban Socioeconomic Growth

The correlation coefficients for urbanization data and atmospheric UHII from 1981 to 2019 were greater than 0.78 ($p < 0.01$), indicating a strong relationship between socioeconomic development indicators and atmospheric UHII (Table 1).

Table 1. Analysis of the relationship between urban development indicators and UHII.

		Built-Up	UR ¹	Population	GDP	PD ²
UHII	Pearson correlation	0.824 **	0.824 **	0.857 **	0.788 **	0.788 **
	Sig. (2-tailed)	0.000	0.000	0.000	0.000	0.000
	N/year (1981–2019)	39	39	39	39	39

¹ UR is urbanization rate; ² PD is population density; ** correlation is significant at the 0.01 level.

The urbanization indicators (built-up area, population, urbanization rate, population density, and GDP) were chosen for further linear regression analysis between them and UHII. The results demonstrated a significant ($p < 0.01$) positive linear correlation between UHII and urbanization indicators (Table 2), as indicated by a p-value less than 0.01. Therefore, it is possible to conclude that the urbanization process increased the UHI effect.

Table 2. Linear regression analysis of the UHII and urban development indicators.

Indicators	Regression Model *	R2	CC *
Population (ten thousand)	$Y = 0.0036x - 0.7464$	0.73	0.86
Built-up area (km ²)	$Y = 0.0031x - 0.3505$	0.68	0.82
Urbanization rate (%)	$Y = 0.0362x - 1.673$	0.63	0.82
Population density (per km ²)	$Y = 0.0019x - 1.4726$	0.67	0.79
GDP	$Y = 0.0001x - 0.0358$	0.62	0.78

* Y stands for UHII. CC * is the correlation coefficient.

In the meantime, based on the results in Table 2, we can predict that a 100 km² increase in the urban area of Zhengzhou will result in a 0.31 °C increase in UHII. Moreover, a one million increase in population will result in a 0.36 °C increase in UHII. The UHI intensity may increase by 1.67 °C by 2035, based on the predicted results of the population growth trend.

Studies have shown synergistic effects with heat waves [39], which are also responsible for daytime UHI peaking in summer (part 4.2), while related studies have also shown that natural factors have a more significant impact on environmental climate comfort in human settlements than anthropogenic ones, and that the great challenges of climate change, rapid urbanization, economic growth, and demographic changes could plunge China into a future struggle against urban warming [40].

The analysis results of urban growth and atmospheric UHII (Figure 6) indicate that the growth rate of urban built-up areas was relatively slow until 2000. However, the UCR index increased rapidly after 2000, indicating that the urbanized area gradually grew and replaced the non-urbanized areas. There is a significant positive correlation between UHII and UCR. This indicates that the heat island effect is more pronounced the larger the urban built-up area.

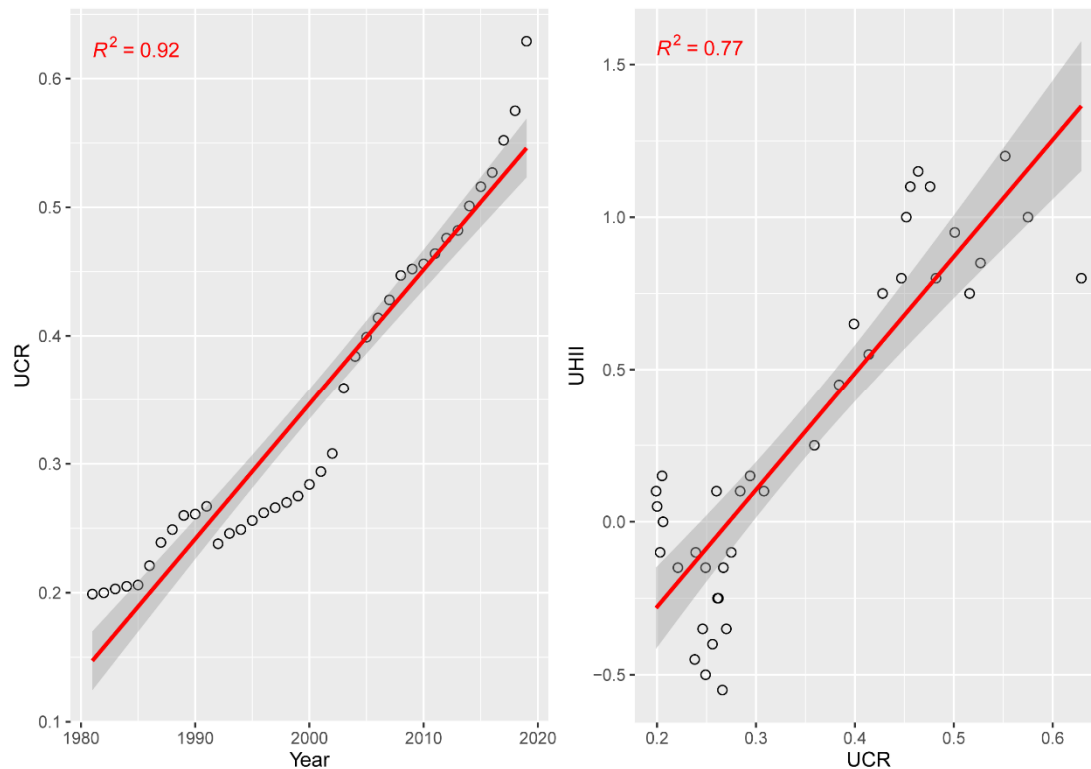


Figure 6. The plot of the urban compactness ratio (UCR) over the past 39 years versus time (left) and linear regression analysis of UCR to UHII (right).

5. Discussion

5.1. Urbanization Roles in Climate Change

In this survey, the present study analyzed atmospheric UHI changes in Zhengzhou characteristics based on long-term observed meteorological data for the past 39 years. The study's findings revealed a warming trend in urban and rural areas (Figure 2), but the increase in urban areas was noticeably greater than in rural areas (Figure 2). The results of other studies also support this urban climate trend result [35,41,42]. The causes of this could be attributed to two factors: First, as a result of global warming, both urban and rural areas worldwide are experiencing significant temperature increases and an increase in the frequency of extreme weather events. However, explained from a physical standpoint, the urbanization process replaces the surface of the original area, changing the physical properties, especially the heat capacity of the surface structure [43]. Built-up urban areas absorb more heat than undeveloped areas, increasing temperature. At the same time, built-up areas reduce the evaporation capacity of the city, and the surfaces of buildings, concrete, asphalt, etc., in built-up areas cannot evaporate compared to urban vegetated areas and water bodies, which also leads to an increase in urban temperature [44]. Additionally, the increase in anthropogenic heat in urban areas also contributes to warming. These are the primary reasons for Zhengzhou's escalating urban climate change.

It is noteworthy that the atmospheric UHI effect in the study area had a turning point at the turn of the century (Figure 3). This is because temperatures between urban and rural areas were close during the low rate of urbanization between 1989 and 2000. Urban areas,

however, rapidly warmed after 2000, and the UHII gradually rose. This is supported by the findings of the analysis between the UHII and urban expansion indicators, which show that the process of urbanization significantly contributes to the urban heat island effect. The atmospheric UHII changes correlate with socioeconomic data (Table 1), such as population, urbanization rate, population density, and GDP.

Urbanization indicators such as the increase in population are the increase of built-up areas in urban areas, and the increase of population density is also the increase in building density (residential areas of high-rise buildings). On the one hand, the heat capacity of the built-up areas produces changes, such as the influence of building materials on temperature; on the other hand, the increase of anthropogenic heat sources (air conditioning use in summer, motor vehicles, etc.), all contribute to the increase of the overall temperature of the city, thus aggravating the urban heat island effect. At the same time, some human activities in the city produce industrial pollutants (PM_{2.5}, photochemical smog, etc.), which produce chemical reactions near the surface and also lead to changes in the thermal properties of aerosols, thus aggravating the heat island effect [45–47].

5.2. UHI and Urban Expansion

This study showed a positive correlation between the presence of UHI and urban sprawl, as evidenced by the analysis of urban sprawl based on the UCR indicator (Figure 6). This result is consistent with previous studies on land use/land cover (LULC) change and the heat island effect [23,26,36], which provides strong evidence that urbanization processes contribute to UHI based on surface temperature and air temperature. Previous studies in Zhengzhou have also shown that replacing permeable land (arable and forest land, etc.) with impermeable urban surfaces manifests urban sprawl [23,36]. Studies have shown that urban heat zones are generally located mostly in built-up areas, while cold islands are generally located in green and watery areas. Previous studies have also shown that the urbanization pattern of Zhengzhou is expanding from the center outward, leading to the spread of urban heat islands from the center to the urban periphery, resulting in the city being filled with built-up areas [26]. Therefore, it is also leading to higher temperatures in urban areas than in the surrounding areas. Nevertheless, the impervious surface reduces the evaporation capacity of the city [48,49], leading to higher urban temperatures. This is the same conclusion for Zhengzhou as mentioned in other urban heat island studies [50–53].

5.3. Policy-Driven Urbanization Process—Indirect Factors

The built-up area of Zhengzhou, from the original 65 km² (1981) to 651.3 km² (2019), is not only related to the overall socioeconomic development of China but also the urbanization policy [54–56]. The rapid development of Zhengzhou after 2000, with the successive national policies, for instance, in 2002, the new city construction (e.g., CBD) was started. The Central Plains Economic Zone was approved in 2012, which is the national strategy for developing the central region. The support of the Central Plains Urban Agglomeration in 2018 led to the development of the Central Plains Urban Agglomeration, with Zhengzhou as the center. The National Central City in 2018 further established Zhengzhou's status as a driving force for the development of the surrounding area. Through these policies, from 1981–2019, Zhengzhou's built-up area has expanded tenfold, its population has increased 2.26 times, and the scale of the city has grown rapidly, not only in the new city but also in the old town, turning it into the high-density mega-city it is today.

5.4. Countermeasures and Outlooks

Urban development has replaced much of the vegetated landscape with built structures and impervious surfaces, altering the near-surface climate and increasing temperatures. Urban warming is closely related to the influence of buildings, and studies have shown that physical variables such as building size, population density, vegetation cover, texture, and surface color significantly affect energy use [57]. The surface temperature increases with building height, and building orientation also affects temperature [58]. The

results of building density on surface temperature for 21 cities in China show that the effect of building density on LST is more significant in dry climates compared to humid climates. The spatial variability of the effects [59] and the heat island effect affect building energy consumption, and studies have shown that UHI intensity can increase the sensible cooling load of residential buildings [60–62]. In some countries, the negative impact of urban development on the heat island effect has been fought. For example, Canada has implemented urban cooling strategies based on natural solutions to mitigate the heat island effect by implementing green roofs and increasing vegetation [63]. In Beijing, China, urban thermal environments are improved through an urban ventilation corridor program [64]. Numerous studies of urban cooling have shown that reflective and green roofs can reduce the surface temperature of roofs [65–67], thereby reducing the corresponding apparent atmospheric heat flux. Increasing the albedo of urban environments [68–71], using cooling materials, and expanding green spaces [72–76] in cities to use natural radiators to dissipate excess heat are effective ways to mitigate urban heat islands.

From the results of this study, we can see that, with urbanization, the city is becoming warmer, and the urban heat island intensity is increasing. Although partly attributed to the influence of the general context of global warming, the urban warming trend is significantly greater than the temperature increase in the suburbs, and the frequency of heat waves and extreme weather in recent years show that we must continue to take action in the construction of future cities to mitigate the urban heat island effect and urban warming trend. Combined with the study, we recommend (1) emphasizing policy guidance, and, in the construction of future cities, urban planners and policymakers should pay attention to the construction of cool cities; (2) strengthening the construction of urban blue-green infrastructure; urban blue-green infrastructure is an urban cool island, and the evapotranspiration of blue-green space plays an important role in mitigating the urban thermal environment; (3) increasing surface greenery/vegetation such as green roofs and vertical greening and increasing surface reflectivity such as cooling pavement materials or cool infrastructure, so as to change the thermal properties to mitigate and reduce the urban heat island effect.

6. Conclusions

This study applied a comprehensive approach to characterize the urban heat island. First, we examined the temporal variation of UHI intensity by applying 39 years (1981–2019) of meteorological data from the study area on annual, seasonal, daytime, and nighttime bases. During the study period, the annual mean temperature in Zhengzhou City increased by 0.67 °C per decade. The analysis of the urban compactness ratio (UCR) indicated that urbanization contributes to the warming trend in Zhengzhou. Second, the socioeconomic development indicators (population, urbanization rate, population density, and built-up area) from 1981 to 2019 were used as indirect factors to examine their correlation with UHI intensity. By using this comprehensive method in Zhengzhou city. We summarized the temporal UHI characteristics:

- (1) UHI intensity increases with time and urban expansion magnitude.
- (2) Renewed evidence shows the changing characteristics of urban heat islands in the Northern Hemisphere. Summer has the highest UHI intensity, spring is the second, and winter is the weakest. Nocturnal UHI intensity was more significant than daytime.
- (3) The urban development indicators (population, urbanization rate, population density, UCR) are all significant factors contributing to the UHI effect.

This research offers a suitable approach and evaluates the UHI intensity variation within a long-term period, which could fulfill the drawback of the remote sensing method that could not present changes in the time scale. Additionally, the long-term urban socio-economic development indicators provide an additional way to characterize the UHI phenomenon.

Author Contributions: Conceptualization, H.L., H.M., and S.J.; methodology, H.L.; software, H.L.; resources, H.M. and G.T.; writing—original draft preparation, H.L. and H.M.; writing—review and editing, H.L., Y.L., and S.J.; visualization, S.J. and H.L. All authors have read and agreed to the published version of the manuscript.

Funding: This research was funded by “Henan Province Young Talent Support Project” (2019HYTP033), Meteorological disaster risk assessment and microclimate simulation and “Henan Overseas Expertise Introduction Center for Discipline Innovation”.

Data Availability Statement: The data presented in this study are available on request from the first author.

Acknowledgments: The authors would like to thank Huawei Li’s previous Ph.D. thesis, “Characteristics, effects and mitigation of urban heat island in developing urban regions.” We thank the support of the Hungarian University of Agriculture and Life Sciences. Moreover, the authors would like to thank the support of the International Joint Laboratory of Landscape Architecture, Henan Agricultural University, for their infinite help.

Conflicts of Interest: The authors declare no conflict of interest.

Appendix A

Table A1. Zhengzhou national weather station LCZ.

Year	LCZ Type	Aerial Images
1988	LCZ D-Agriculture land	
2005	LCZ-6 Open low-rise	

Table A1. Cont.

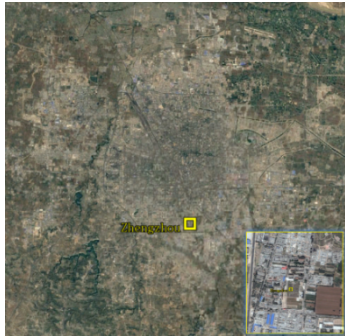
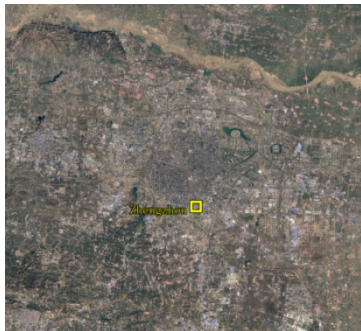
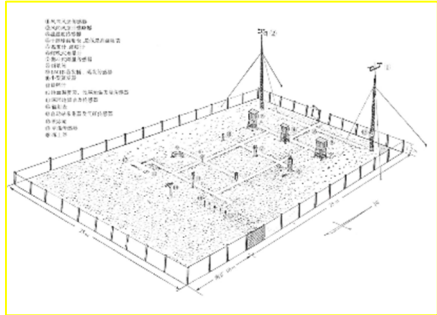
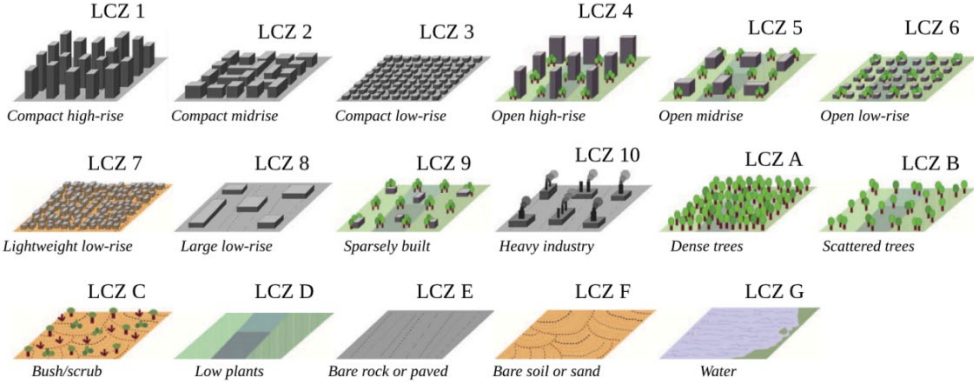
Year	LCZ Type	Aerial Images
2007	LCZ-4 Open mid-rise 	
2019	LCZ-1 Open high-rise 	
National Standard Station model		
<p style="text-align: center;">Aerial map Reference model from 《Specifications for surface meteorological observation》 QX/T 61-2007 National Standard</p>		
		
<p>Local climate zone types (Stewart & Oke 2012)</p>		

Table A2. Xinzheng national weather station LCZ.

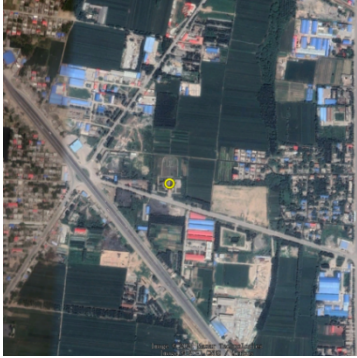
Year	LCZ Type	Aerial Images
1988	LCZ D-Agriculture land	
2009	LCZ D-Agriculture land	
2013	LCZ-9 Sparsely built	
2019	LCZ-4 Open low-rise	

Table A3. Statistics of annual data of urban development in Zhengzhou city from 1981–2019 (data source: Zhengzhou Bureau of Statistics Department).

Year	Built-Up/km ²	Citizens/Million	* Urbanization Rate/%	Population Density/km ²	GDP/CNY
1981	65	4.58	35	616	31.1
1982	66	4.67	35.8	628	33.3
1983	67.8	4.74	36.7	637	37.5
1984	69.3	4.8	37.6	645	43.3
1985	70.2	4.85	38.4	652	49.7
1986	80.5	4.91	39.3	660	53.4
1987	94.2	5.00	40.1	672	66.3
1988	102	5.10	41	686	81.5
1989	110.9	5.21	41.9	700	97.8
1990	112	5.57	42.7	749	116.4
1991	117.2	5.65	43.9	759	138.7
1992	93.1	5.70	45.2	767	167.4
1993	99.5	5.81	46.4	781	218.4
1994	101.9	5.88	47.7	791	287.9
1995	108.3	6.00	48.9	806	386.4
1996	112.8	6.07	50.1	816	498.2
1997	116.2	6.14	51.4	826	566
1998	119.8	6.22	52.6	836	610
1999	124.5	6.31	53.9	848	632.9
2000	133.2	6.65	55.1	894	728.4
2001	142.4	6.77	55.5	909	815.8
2002	156.4	6.87	56	924	913.9
2003	212.4	6.97	57	937	1074.1
2004	243.3	7.08	57.9	951	1335.2
2005	262	7.16	59.2	962	1660.6
2006	282	7.24	60.2	973	2007.8
2007	302	7.35	61.3	988	2486.7
2008	328.7	7.43	62.3	999	3012.9
2009	336.7	7.52	63.4	1010	3305.9
2010	342.7	8.66	63.6	1163	4029.3
2011	354.7	8.85	64.8	1189	4954.1
2012	373	9.03	66.3	1213	5517.1
2013	382.7	9.19	67.1	1234	6197.4
2014	412.7	9.37	68.3	1259	6777
2015	437.6	9.56	69.7	1285	7311.5
2016	456.6	9.72	71	1306	8114
2017	500.8	9.88	72.2	1327	9193.8
2018	543.9	10.13	73.4	1361	10,670.1
2019	651.3	10.35	74.6	1390	11,589.7

* The urbanization rate is a measure of urbanization, generally using a demographic indicator, which is the proportion of the urban population to the total population (including agricultural and non-agricultural).

References

1. Droughts in Europe in July 2022: Almost Half of the EU + UK Territory at Risk. Available online: https://joint-research-centre.ec.europa.eu/jrc-news/droughts-europe-july-2022-almost-half-eu-uk-territory-risk-2022-07-18_en (accessed on 28 August 2022).
2. United Nations. *World Population Prospects 2019–Volume II: Demographic Profiles*; UN: New York, NY, USA, 2020; ISBN 978-92-1-004643-5.
3. Oke, T.R. *Boundary Layer Climates*; Taylor & Francis: Oxford, UK, 2002; ISBN 978-1-134-95133-8.
4. Kotharkar, R.; Ramesh, A.; Bagade, A. Urban Heat Island Studies in South Asia: A Critical Review. *Urban Clim.* **2018**, *24*, 1011–1026. [CrossRef]
5. Phelan, P.E.; Kaloush, K.; Miner, M.; Golden, J.; Phelan, B.; Silva, H.; Taylor, R.A. Urban Heat Island: Mechanisms, Implications, and Possible Remedies. *Annu. Rev. Environ. Resour.* **2015**, *40*, 285–307. [CrossRef]
6. Deilami, K.; Kamruzzaman, M.; Liu, Y. Urban Heat Island Effect: A Systematic Review of Spatio-Temporal Factors, Data, Methods, and Mitigation Measures. *Int. J. Appl. Earth Obs. Geoinf.* **2018**, *67*, 30–42. [CrossRef]

7. Ward, K.; Lauf, S.; Kleinschmit, B.; Endlicher, W. Heat Waves and Urban Heat Islands in Europe: A Review of Relevant Drivers. *Sci. Total Environ.* **2016**, *569–570*, 527–539. [[CrossRef](#)]
8. Gaffin, S.R.; Rosenzweig, C.; Khanbilvardi, R.; Parshall, L.; Mahani, S.; Glickman, H.; Goldberg, R.; Blake, R.; Slosberg, R.B.; Hillel, D. Variations in New York City's Urban Heat Island Strength over Time and Space. *Theor. Appl. Clim.* **2008**, *94*, 1–11. [[CrossRef](#)]
9. Kataoka, K.; Matsumoto, F.; Ichinose, T.; Taniguchi, M. Urban Warming Trends in Several Large Asian Cities over the Last 100 Years. *Sci. Total Environ.* **2009**, *407*, 3112–3119. [[CrossRef](#)]
10. Hong, J.-W.; Hong, J.; Kwon, E.E.; Yoon, D.K. Temporal Dynamics of Urban Heat Island Correlated with the Socio-Economic Development over the Past Half-Century in Seoul, Korea. *Environ. Pollut.* **2019**, *254*, 112934. [[CrossRef](#)]
11. Ren, G.; Zhou, Y.; Chu, Z.; Zhou, J.; Zhang, A.; Guo, J.; Liu, X. Urbanization Effects on Observed Surface Air Temperature Trends in North China. *J. Clim.* **2008**, *21*, 1333–1348. [[CrossRef](#)]
12. Manoli, G.; Fatichi, S.; Schläpfer, M.; Yu, K.; Crowther, T.W.; Meili, N.; Burlando, P.; Katul, G.G.; Bou-Zeid, E. Magnitude of Urban Heat Islands Largely Explained by Climate and Population. *Nature* **2019**, *573*, 55–60. [[CrossRef](#)]
13. Howard, L. *The Climate of London: Deduced from Meteorological Observations*; Cambridge University Press: Cambridge, UK, 2012; ISBN 978-1-108-04952-8.
14. Unger, J. Intra-Urban Relationship between Surface Geometry and Urban Heat Island: Review and New Approach. *Clim. Res.* **2004**, *27*, 253–264. [[CrossRef](#)]
15. Oke, T.R. The Distinction between Canopy and Boundary-layer Urban Heat Islands. *Atmosphere* **1976**, *14*, 268–277. [[CrossRef](#)]
16. Oke, T.R. Street Design and Urban Canopy Layer Climate. *Energy Build.* **1988**, *11*, 103–113. [[CrossRef](#)]
17. Ooka, R.; Sato, T.; Harayama, K.; Murakami, S.; Kawamoto, Y. Thermal Energy Balance Analysis of the Tokyo Metropolitan Area Using a Mesoscale Meteorological Model Incorporating an Urban Canopy Model. *Bound.-Layer Meteorol.* **2011**, *138*, 77–97. [[CrossRef](#)]
18. Park, B.-J.; Kim, Y.-H.; Min, S.-K.; Kim, M.-K.; Choi, Y.; Boo, K.-O.; Shim, S. Long-Term Warming Trends in Korea and Contribution of Urbanization: An Updated Assessment: Urbanization Contribution in Korea. *J. Geophys. Res. Atmos.* **2017**, *122*, 10637–10654. [[CrossRef](#)]
19. Xiong, Y.; Huang, S.; Chen, F.; Ye, H.; Wang, C.; Zhu, C. The Impacts of Rapid Urbanization on the Thermal Environment: A Remote Sensing Study of Guangzhou, South China. *Remote Sens.* **2012**, *4*, 2033–2056. [[CrossRef](#)]
20. Chapman, S.; Watson, J.E.M.; Salazar, A.; Thatcher, M.; McAlpine, C.A. The Impact of Urbanization and Climate Change on Urban Temperatures: A Systematic Review. *Landsc. Ecol.* **2017**, *32*, 1921–1935. [[CrossRef](#)]
21. Yu, Z.; Yao, Y.; Yang, G.; Wang, X.; Vejre, H. Spatiotemporal Patterns and Characteristics of Remotely Sensed Region Heat Islands during the Rapid Urbanization (1995–2015) of Southern China. *Sci. Total Environ.* **2019**, *674*, 242–254. [[CrossRef](#)]
22. Sun, S. An Analysis on Planning Paradigms and the Evolution of Urban Planning in China. *UPI* **2019**, *34*, 1–7. [[CrossRef](#)]
23. Min, M.; Zhao, H.; Miao, C. Spatio-Temporal Evolution Analysis of the Urban Heat Island: A Case Study of Zhengzhou City, China. *Sustainability* **2018**, *10*, 1992. [[CrossRef](#)]
24. Zhao, H.; Zhang, H.; Miao, C.; Ye, X.; Min, M. Linking Heat Source–Sink Landscape Patterns with Analysis of Urban Heat Islands: Study on the Fast-Growing Zhengzhou City in Central China. *Remote Sens.* **2018**, *10*, 1268. [[CrossRef](#)]
25. Zhao, H.; Ren, Z.; Tan, J. The Spatial Patterns of Land Surface Temperature and Its Impact Factors: Spatial Non-Stationarity and Scale Effects Based on a Geographically-Weighted Regression Model. *Sustainability* **2018**, *10*, 2242. [[CrossRef](#)]
26. Yang, H.; Xi, C.; Zhao, X.; Mao, P.; Wang, Z.; Shi, Y.; He, T.; Li, Z. Measuring the Urban Land Surface Temperature Variations Under Zhengzhou City Expansion Using Landsat-Like Data. *Remote Sens.* **2020**, *12*, 801. [[CrossRef](#)]
27. Khan, S.; Gul, S.; Li, W. Remote Sensing Evaluation of Land Surface Temperature and Urban Area Expansion in Zhengzhou City during 2013–2015. *Nat. Appl. Sci. Int. J. (NASIJ)* **2021**, *2*, 39–55. [[CrossRef](#)]
28. Yang, Y.; Song, F.; Ma, J.; Wei, Z.; Song, L.; Cao, W. Spatial and Temporal Variation of Heat Islands in the Main Urban Area of Zhengzhou under the Two-Way Influence of Urbanization and Urban Forestry. *PLoS ONE* **2022**, *17*, e0272626. [[CrossRef](#)]
29. Stewart, I.D.; Oke, T.R. Local Climate Zones for Urban Temperature Studies. *Bull. Am. Meteorol. Soc.* **2012**, *93*, 1879–1900. [[CrossRef](#)]
30. Lelovics, E.; Unger, J.; Gál, T.; Gál, C. Design of an Urban Monitoring Network Based on Local Climate Zone Mapping and Temperature Pattern Modelling. *Clim. Res.* **2014**, *60*, 51–62. [[CrossRef](#)]
31. Zhou, X.; Okaze, T.; Ren, C.; Cai, M.; Ishida, Y.; Watanabe, H.; Mochida, A. Evaluation of Urban Heat Islands Using Local Climate Zones and the Influence of Sea-Land Breeze. *Sustain. Cities Soc.* **2020**, *55*, 102060. [[CrossRef](#)]
32. Dian, C.; Pongrácz, R.; Incze, D.; Bartholy, J.; Talamon, A. Analysis of the Urban Heat Island Intensity Based on Air Temperature Measurements in a Renovated Part of Budapest (Hungary). *Geogr. Pannonica* **2019**, *23*, 277–288. [[CrossRef](#)]
33. Chen, Y. Derivation of the Functional Relations between Fractal Dimension of and Shape Indices of Urban Form. *Comput. Environ. Urban Syst.* **2011**, *35*, 442–451. [[CrossRef](#)]
34. Haggett, P.; Cliff, A.D.; Frey, A. *Locational Analysis in Human Geography*; Arnold: London, UK, 1977; Volume 2.
35. Hansen, J.; Ruedy, R.; Sato, M.; Lo, K. Global Surface Temperature Change. *Rev. Geophys.* **2010**, *48*, 1–29. [[CrossRef](#)]
36. Mu, B.; Mayer, A.L.; He, R.; Tian, G. Land Use Dynamics and Policy Implications in Central China: A Case Study of Zhengzhou. *Cities* **2016**, *58*, 39–49. [[CrossRef](#)]
37. Dimoudi, A.; Nikolopoulou, M. Vegetation in the Urban Environment: Microclimatic Analysis and Benefits. *Energy Build.* **2003**, *35*, 69–76. [[CrossRef](#)]

38. Chen, J.; Jin, S.; Du, P. Roles of Horizontal and Vertical Tree Canopy Structure in Mitigating Daytime and Nighttime Urban Heat Island Effects. *Int. J. Appl. Earth Obs. Geoinf.* **2020**, *89*, 102060. [[CrossRef](#)]
39. Zhou, C.; Zhang, D.; Cao, Y.; Wang, Y.; Zhang, G. Spatio-Temporal Evolution and Factors of Climate Comfort for Urban Human Settlements in the Guangdong–Hong Kong–Macau Greater Bay Area. *Front. Environ. Sci.* **2022**, *10*, 1001064. [[CrossRef](#)]
40. He, B.-J.; Wang, J.; Zhu, J.; Qi, J. Beating the Urban Heat: Situation, Background, Impacts and the Way Forward in China. *Renew. Sustain. Energy Rev.* **2022**, *161*, 112350. [[CrossRef](#)]
41. Chow, W.T.L.; Roth, M. Temporal Dynamics of the Urban Heat Island of Singapore. *Int. J. Climatol.* **2006**, *26*, 2243–2260. [[CrossRef](#)]
42. Lee, T.-W.; Lee, J.Y.; Wang, Z.-H. Scaling of the Urban Heat Island Intensity Using Time-Dependent Energy Balance. *Urban Clim.* **2012**, *2*, 16–24. [[CrossRef](#)]
43. Bowen, I.S. The Ratio of Heat Losses by Conduction and by Evaporation from Any Water Surface. *Phys. Rev.* **1926**, *27*, 779–787. [[CrossRef](#)]
44. Qiu, G.; Li, H.; Zhang, Q.; Chen, W.; Liang, X.; Li, X. Effects of Evapotranspiration on Mitigation of Urban Temperature by Vegetation and Urban Agriculture. *J. Integr. Agric.* **2013**, *12*, 1307–1315. [[CrossRef](#)]
45. Zhong, C.; Chen, C.; Liu, Y.; Gao, P.; Li, H. A Specific Study on the Impacts of PM2.5 on Urban Heat Islands with Detailed In Situ Data and Satellite Images. *Sustainability* **2019**, *11*, 7075. [[CrossRef](#)]
46. Zhang, D.; Zhou, C.; He, B.-J. Spatial and Temporal Heterogeneity of Urban Land Area and PM2.5 Concentration in China. *Urban Clim.* **2022**, *45*, 101268. [[CrossRef](#)]
47. Yang, J.; Xin, J.; Zhang, Y.; Xiao, X.; Xia, J.C. Contributions of Sea–Land Breeze and Local Climate Zones to Daytime and Nighttime Heat Island Intensity. *npj Urban Sustain.* **2022**, *2*, 12. [[CrossRef](#)]
48. Stabler, L.B.; Martin, C.A.; Brazel, A.J. Microclimates in a Desert City Were Related to Land Use and Vegetation Index. *Urban For. Urban Green.* **2005**, *3*, 137–147. [[CrossRef](#)]
49. Li, X.-X.; Liu, X. Effect of Tree Evapotranspiration and Hydrological Processes on Urban Microclimate in a Tropical City: A WRF/SLUCM Study. *Urban Clim.* **2021**, *40*, 101009. [[CrossRef](#)]
50. Xu, H.; Ding, F.; Wen, X. Urban Expansion and Heat Island Dynamics in the Quanzhou Region, China. *IEEE J. Sel. Top. Appl. Earth Obs. Remote Sens.* **2009**, *2*, 74–79. [[CrossRef](#)]
51. Qiao, Z.; Tian, G.; Zhang, L.; Xu, X. Influences of Urban Expansion on Urban Heat Island in Beijing during 1989–2010. *Adv. Meteorol.* **2014**, *2014*, e187169. [[CrossRef](#)]
52. Li, Y.; Zhang, H.; Kainz, W. Monitoring Patterns of Urban Heat Islands of the Fast-Growing Shanghai Metropolis, China: Using Time-Series of Landsat TM/ETM+ Data. *Int. J. Appl. Earth Obs. Geoinf.* **2012**, *19*, 127–138. [[CrossRef](#)]
53. Shen, H.; Huang, L.; Zhang, L.; Wu, P.; Zeng, C. Long-Term and Fine-Scale Satellite Monitoring of the Urban Heat Island Effect by the Fusion of Multi-Temporal and Multi-Sensor Remote Sensed Data: A 26-Year Case Study of the City of Wuhan in China. *Remote Sens. Environ.* **2016**, *172*, 109–125. [[CrossRef](#)]
54. Kamal-Chaoui, L.; Leeman, E.; Rufei, Z. *Urban Trends and Policy in China*; OECD Publishing: Paris, France, 2009. [[CrossRef](#)]
55. Wei, H.; Li, L.; Nian, M. China’s Urbanization Strategy and Policy During the 14th Five-Year Plan Period. *Chin. J. Urban Environ. Stud.* **2021**, *9*, 2150002. [[CrossRef](#)]
56. Ding, C.; Zhao, X. Urbanization in Japan, South Korea, and China: Policy and Reality. In *The Oxford Handbook of Urban Economics and Planning*; Brooks, N., Donaghy, K., Knaap, G., Eds.; Oxford University Press: Oxford, UK, 2011; pp. 906–931. ISBN 978-0-19-538062-0.
57. Faroughi, M.; Karimimoshaver, M.; Aram, F.; Solgi, E.; Mosavi, A.; Nabipour, N.; Chau, K.-W. Computational Modeling of Land Surface Temperature Using Remote Sensing Data to Investigate the Spatial Arrangement of Buildings and Energy Consumption Relationship. *Eng. Appl. Comput. Fluid Mech.* **2020**, *14*, 254–270. [[CrossRef](#)]
58. Alexander, C. Influence of the Proportion, Height and Proximity of Vegetation and Buildings on Urban Land Surface Temperature. *Int. J. Appl. Earth Obs. Geoinf.* **2021**, *95*, 102265. [[CrossRef](#)]
59. Song, J.; Chen, W.; Zhang, J.; Huang, K.; Hou, B.; Prishchepov, A.V. Effects of Building Density on Land Surface Temperature in China: Spatial Patterns and Determinants. *Landsc. Urban Plan.* **2020**, *198*, 103794. [[CrossRef](#)]
60. Salvati, A.; Roura, H.C.; Cecere, C. Assessing the Urban Heat Island and Its Energy Impact on Residential Buildings in Mediterranean Climate: Barcelona Case Study. *Energy Build.* **2017**, *146*, 38–54. [[CrossRef](#)]
61. Santamouris, M. On the Energy Impact of Urban Heat Island and Global Warming on Buildings. *Energy Build.* **2014**, *82*, 100–113. [[CrossRef](#)]
62. Santamouris, M.; Cartalis, C.; Synnefa, A.; Kolokotsa, D. On the Impact of Urban Heat Island and Global Warming on the Power Demand and Electricity Consumption of Buildings—A Review. *Energy Build.* **2015**, *98*, 119–124. [[CrossRef](#)]
63. Hayes, A.T.; Jandaghian, Z.; Lacasse, M.A.; Gaur, A.; Lu, H.; Laouadi, A.; Ge, H.; Wang, L. Nature-Based Solutions (NBSs) to Mitigate Urban Heat Island (UHI) Effects in Canadian Cities. *Buildings* **2022**, *12*, 925. [[CrossRef](#)]
64. Bing, D.; Zhaoyin, Y.; Wupeng, D.; Xiaoyi, F.; Yonghong, L.; Chen, C.; Yan, L. Cooling the City with “Natural Wind”: Construction Strategy of Urban Ventilation Corridors in China. *IOP Conf. Ser. Earth Environ. Sci.* **2021**, *657*, 012009. [[CrossRef](#)]
65. Santamouris, M. Cooling the Cities—A Review of Reflective and Green Roof Mitigation Technologies to Fight Heat Island and Improve Comfort in Urban Environments. *Sol. Energy* **2014**, *103*, 682–703. [[CrossRef](#)]
66. Dwivedi, A.; Mohan, B.K. Impact of Green Roof on Micro Climate to Reduce Urban Heat Island. *Remote Sens. Appl. Soc. Environ.* **2018**, *10*, 56–69. [[CrossRef](#)]

67. Shao, H.; Song, P.; Mu, B.; Tian, G.; Chen, Q.; He, R.; Kim, G. Assessing City-Scale Green Roof Development Potential Using Unmanned Aerial Vehicle (UAV) Imagery. *Urban For. Urban Green.* **2021**, *57*, 126954. [[CrossRef](#)]
68. Bhattacharya, B.K.; Mallick, K.; Padmanabhan, N.; Patel, N.K.; Parihar, J.S. Retrieval of Land Surface Albedo and Temperature Using Data from the Indian Geostationary Satellite: A Case Study for the Winter Months. *Int. J. Remote Sens.* **2009**, *30*, 3239–3257. [[CrossRef](#)]
69. Erell, E.; Pearlmutter, D.; Boneh, D.; Kutiel, P.B. Effect of High-Albedo Materials on Pedestrian Heat Stress in Urban Street Canyons. *Urban Clim.* **2014**, *10*, 367–386. [[CrossRef](#)]
70. Taha, H. Urban Climates and Heat Islands: Albedo, Evapotranspiration, and Anthropogenic Heat. *Energy Build.* **1997**, *25*, 99–103. [[CrossRef](#)]
71. Xu, X.; Asawa, T.; Kobayashi, H. Narrow-to-Broadband Conversion for Albedo Estimation on Urban Surfaces by UAV-Based Multispectral Camera. *Remote Sens.* **2020**, *12*, 2214. [[CrossRef](#)]
72. Zhang, Z.; Lv, Y.; Pan, H. Cooling and Humidifying Effect of Plant Communities in Subtropical Urban Parks. *Urban For. Urban Green.* **2013**, *12*, 323–329. [[CrossRef](#)]
73. Du, H.; Song, X.; Jiang, H.; Kan, Z.; Wang, Z.; Cai, Y. Research on the Cooling Island Effects of Water Body: A Case Study of Shanghai, China. *Ecol. Indic.* **2016**, *67*, 31–38. [[CrossRef](#)]
74. Aram, F.; Solgi, E.; Higuera García, E.; Mosavi, A.; Várkonyi-Kóczy, A.R. The Cooling Effect of Large-Scale Urban Parks on Surrounding Area Thermal Comfort. *Energies* **2019**, *12*, 3904. [[CrossRef](#)]
75. Chen, X.; Su, Y.; Li, D.; Huang, G.; Chen, W.; Chen, S. Study on the Cooling Effects of Urban Parks on Surrounding Environments Using Landsat TM Data: A Case Study in Guangzhou, Southern China. *Int. J. Remote Sens.* **2012**, *33*, 5889–5914. [[CrossRef](#)]
76. Shen, Z.-J.; Zhang, B.-H.; Xin, R.-H.; Liu, J.-Y. Examining Supply and Demand of Cooling Effect of Blue and Green Spaces in Mitigating Urban Heat Island Effects: A Case Study of the Fujian Delta Urban Agglomeration (FDUA), China. *Ecol. Indic.* **2022**, *142*, 109187. [[CrossRef](#)]